

Force and conductance during contact formation to a C₆₀ molecule - Supplementary Data -

Nadine Hauptmann¹, Fabian Mohn², Leo Gross², Gerhard Meyer², Thomas Frederiksen³, and Richard Berndt¹

¹Institut für Experimentelle und Angewandte Physik,
Christian-Albrechts-Universität zu Kiel, D-24098 Kiel, Germany

²IBM Research – Zurich, CH-8803 Rüschlikon, Switzerland

³Donostia International Physics Center (DIPC), E-20018 Donostia-San Sebastián,
Spain

E-mail: hauptmann@physik.uni-kiel.de

1. Experimental details

Frequency shift–distance curves were recorded as follows. The current feedback was disabled and the tip was retracted from the surface by several angstroms. The frequency shift Δf and the time-averaged tunneling current I_{avg} were recorded while approaching the tip towards the surface and during the subsequent retraction to its starting position. Curves were acquired with 2000 data points in 60 to 120 s. Since no significant differences were observed between the approach and retraction data, modifications of the tip apex or the molecular orientation during measurements can be excluded. In addition, STM images taken before and after current–distance measurements showed no changes. Furthermore, the intrinsic energy dissipation of the tuning fork did not change significantly during approach and retraction of the tip. As the cantilever, one prong of a

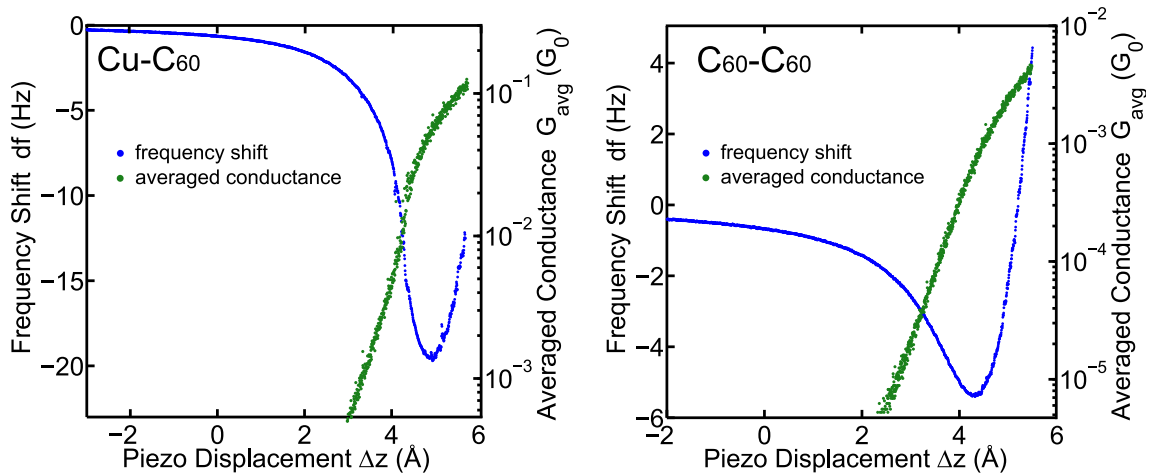


Figure S1. Frequency shift df and time-averaged conductance G_{avg} versus the piezo displacement Δz for the Cu- C_{60} and C_{60} - C_{60} contacts shown in Fig. 1(c) and Fig. 2(h), respectively. The oscillation amplitudes are $A = (3 \pm 0.2) \text{\AA}$ for the Cu- C_{60} contact and $A = (2.5 \pm 0.2) \text{\AA}$ for the C_{60} - C_{60} contact.

tuning fork was used (spring constant $k \approx 1800 \text{ N/m}$) while the second prong was fixed on the piezo scanner. Measurements were performed at oscillation amplitudes between $A = 1 \text{\AA}$ and $A = 3 \text{\AA}$. The amplitude A corresponds to half of the peak-to-peak distance of the oscillation. The uncertainty of the calibration of the used amplitude is $\approx 7\%$. This margin is essentially due to the uncertainty of the calibration of the z-piezo, where $\approx 5\%$ are routinely achieved for small displacements. The bandwidth of the transimpedance amplifier for the tunneling current varies between 7 and 200 kHz depending on the used amplifier gain. The current data was further filtered by a numerical low-pass filter with a cut-off frequency of 8 kHz.

1.1. Extraction of the short-range force

The short-range force F_s can be obtained by subtracting the long-range van-der-Waals force F_l from the total force F . We use a power law to approximate F_l by

$F_l(\Delta z) = a(\Delta z_0 - \Delta z)^b$. The fit parameters depend on the range of the fit. E.g., for the fit range $\Delta z \leq 0 \text{ \AA}$ we find $a = -5.5 \text{ nN/\AA}^b$, $b = -2.3$, and $\Delta z_0 = 7.5 \text{ \AA}$. For $\Delta z \leq -1 \text{ \AA}$ and $\Delta z \leq 1 \text{ \AA}$ we obtain $a = -6.5 \text{ nN/\AA}^b$, $b = -2.34$, $\Delta z_0 = 7.8 \text{ \AA}$ and $a = -2 \text{ nN/\AA}^b$, $b = -1.9$, $\Delta z_0 = 6.3 \text{ \AA}$, respectively. Figure S2 shows the influence on F_s for the different fit ranges. The absolute value of F_s can change by a factor of

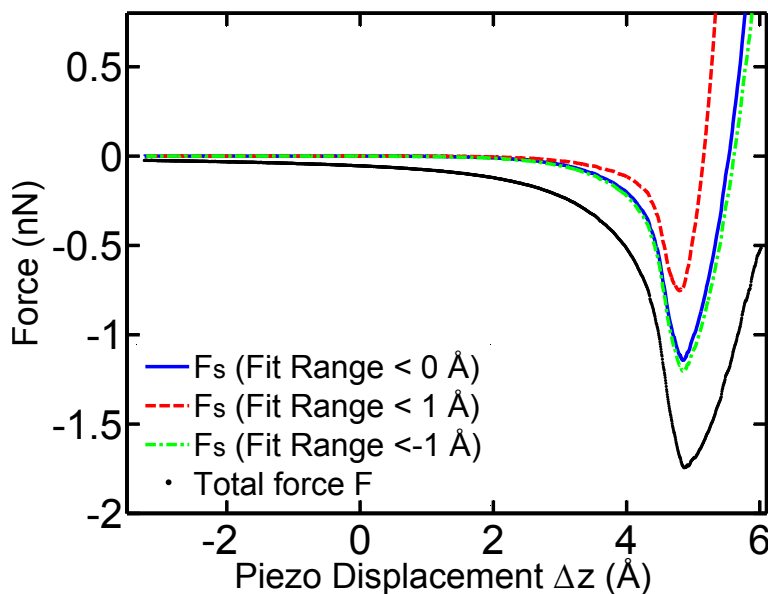


Figure S2. Total force F (dots) and short-range forces F_s (solid, dashed, and dashed-dotted lines) versus the piezo displacement Δz . The three F_s curves are extracted by three long-range force fits with different fit ranges.

2 depending on the fit range. However, the displacement Δz where contact occurs is only weakly influenced by the different long-range force fits. It shifts by $\approx 0.12 \text{ \AA}$ at most. Therefore we did not use F_s for a quantitative comparison. Rather we compare the more robust point of maximal attraction with the point of contact.

2. Simulation of images recorded with C_{60} -tips

The highest occupied molecular orbitals (HOMO) of C_{60} exhibit a large local density of states (LDOS) at the 6:6 bonds, which is known from DFT calculations. Motivated by this result, we modeled the HOMO of a h - C_{60} -tip by a threefold-symmetric pattern of two-dimensional Gaussians [Fig. S3(a)-(c)]. For simplicity it was assumed that only the LDOS of the hexagon which is closest to the surface contributes to the tunneling current. The same approach was used to mimic the lowest unoccupied molecular orbital (LUMO) of h - C_{60} and p - C_{60} on the substrate, which are most intense at the 5:6 bonds [Fig. S3(d-f)]. As images of adsorbed h - C_{60} recorded with a Cu-tip reveal the positions of the bonds, the relative orientation of C_{60} at the tip and the surface were determined from the experiment. For p - C_{60} the situation is less favorable, because the molecule appears circularly symmetric when using a Cu tip. A two-dimensional convolution of

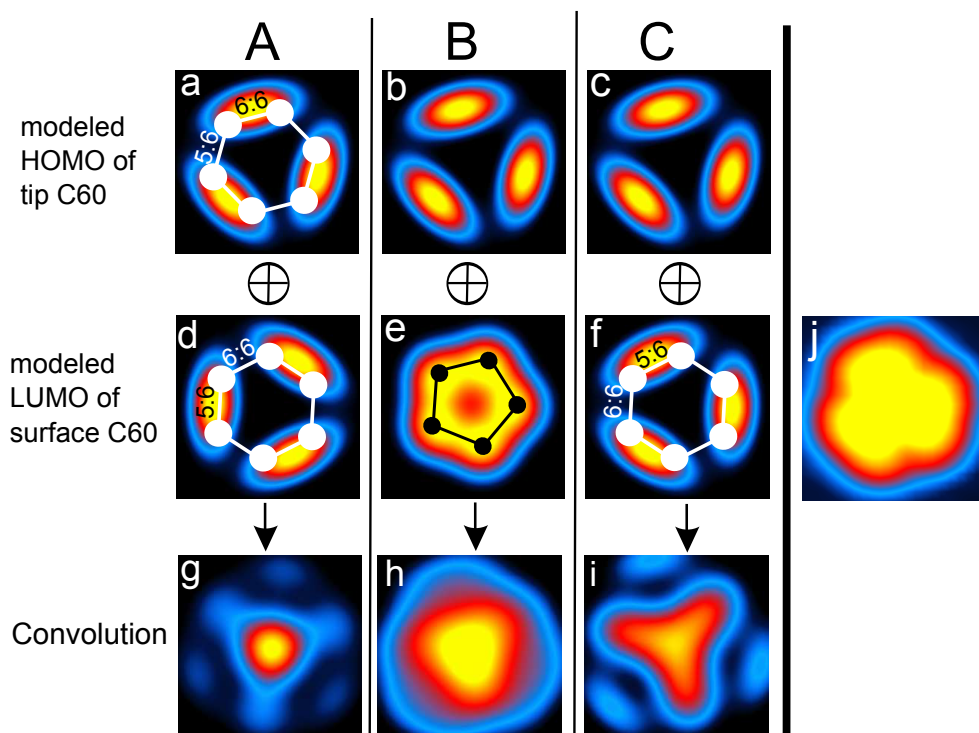


Figure S3. (a–c) Model LDOS of the HOMO of a $h-C_{60}$ -tip hexagon as viewed from the tip. (d–f) Model LDOS of the LUMO of $h-C_{60}$ and $p-C_{60}$ on the surface. (g–i) Two-dimensional convolution of tip and sample LDOS. White hexagons and a black pentagon indicate the molecular orientation as viewed from the tip. A, B, and C refer to the surface regions defined in Figs. 1(b) and Fig. 2(b). (j) Constant-current STM image (-2 V , 0.26 nA , $1.7 \times 1.6\text{ nm}^2$) of a Cu cluster with a C_{60} tip.

these patterns [Figs. 2(e–g) and Figs. S3(g–i)] reproduces the experimental images of $h-C_{60}$ qualitatively very well. The orientation of the C_{60} molecule attached to the tip was determined by scanning a Cu cluster, consisting of a few Cu atoms, with the C_{60} tip. Fig. S3(j) shows the experimental data ($V = -2\text{ V}$). This image is rotated by 180° (about an axis perpendicular to the image plane) compared to that of a C_{60} on the sample surface scanned with a metal tip.